THE JOURNAL OF PHYSICAL CHEMISTRY B LETTERS

**2006,** *110,* 18093−18096
Published on Web 08/29/2006

# Probing Electron Transfer Dynamics at MgO Surfaces by Mg-Atom Desorption

**Alan G. Joly,[†] Matthias Henyk,[†] Kenneth M. Beck,[†] Paolo E. Trevisanutto,[‡] Peter V. Sushko,[‡] Wayne P. Hess,*[,†] and Alexander L. Shluger[‡]**

*Pacific Northwest National Laboratory, P.O. Box 999, Richland, Washington 99352, and Department of Physics and Astronomy, University College London, Gower Street, London WC1E 6BT, U.K.*

*Received: June 29, 2006; In Final Form: August 14, 2006*

Ultraviolet excitation of high surface area MgO films using 4.7 eV femtosecond pulses results in neutral Mg-atom desorption with hyperthermal kinetic energies in the range 0.1−0.4 eV. The Mg-atom hyperthermal energies and power dependences are similar to those previously observed using nanosecond pulsed excitation. Femtosecond two-pulse correlation measurements reveal the existence of different dynamical paths for Mg-atom desorption. One mechanism displays a sub-150 fs time scale and involves the simultaneous or near-simultaneous transition of two electrons to a 3-coordinated $Mg^{2+}$ site. Other paths display picosecond time scales that we associate with dynamics following electron trapping at 3-coordinated $Mg^{2+}$ surface sites.

## 1. Introduction

Electron transfer is a rapid elementary process important in many physical, chemical, and biological systems. Femtosecond spectroscopy has become an important tool to explore short-time dynamics inherent in electron transfer processes in molecular systems.[1−3] However, studying such processes in solids, and at surfaces, still presents formidable challenges due to difficulties in exciting specific electronic states and making direct correlation to the subsequent transfer dynamics. Recent success in understanding the mechanisms of atomic desorption following photoselective surface excitation of wide-gap insulators, such as NaCl and MgO,[4−6] suggest these systems as good candidates for direct exploration of electron transfer dynamics at surfaces.

Photoinduced processes on MgO have been studied extensively using various experimental techniques, such as optical reflectance,[7,8] luminescence,[7,9−12] electron paramagnetic resonance,[13,14] and atomic desorption.[4−6,15,16] These investigations, combined with theoretical calculations,[6] have successfully assigned particular spectroscopic bands with specific surface sites such as corners and steps. In particular, low-coordinated sites at the MgO(001) surface, 3-coordinated corners, kinks, and step corners, and 4-coordinated steps, display optical absorption band maxima located at 4.6 and 5.4 eV, respectively.[7,17−19] These energies are much lower than the 7.8 eV bulk optical band gap such that it is possible to excite low-coordinated surface sites *selectively* without inducing dynamical complications due to bulk electronic processes. For example, excitation of 3-coordinated (3C) surface sites has been shown to induce characteristic photoluminescence and formation of a metastable surface hole center ($O^-$).[13,14]

Recently, emission of hyperthermal neutral Mg and O atoms from photoexcited MgO surfaces has been studied using an ultrasensitive laser detection technique.[4,6] The desorption of neutral Mg and O atoms takes place with characteristic hyperthermal kinetic energies that provide a *unique detection signal* for studying surface dynamics.[4−6] The combination of site-selective photoexcitation, ultrasensitive atom detection, and tractability to ab initio calculation makes MgO an ideal material for investigating surface electron transfer dynamics.

The electronic structure of MgO, before optical excitation, is characterized by strong localization of valence electrons as well as a large band gap between occupied anion (O 2p) and unoccupied cation (Mg 3s) states.[18] Detection of neutral Mg atoms ($Mg^0$) following optical excitation raises intriguing issues that concern the energetics and dynamics of transferring two valence electrons to a single cation site resulting in the reduction of metal ions to neutral atoms ($Mg^{2+} + 2e^- \rightarrow Mg$). It has been suggested recently that hyperthermal Mg- and O-atom desorption can be explained by double-excitation of 3C surface sites or, alternatively, by electron (hole) trapping at 3C magnesium (oxygen) sites and sequential photoexcitation.[4−6,20] In this letter, we use femtosecond pulse-pair excitation to explore ultrafast electron transfer dynamics of low-coordinated MgO surface sites. We measure time-resolved $Mg^0$ desorption and identify unique short-time electron transfer dynamics associated with correlated and uncorrelated electron motion. The observed ultrafast dynamics are related to specific processes predicted by recent ab initio calculations and models developed from results of nanosecond laser desorption studies.[4−6,20]

## 2. Experimental Methods

Laser desorption experiments are performed under ultrahigh vacuum conditions (base pressure $<10^{-9}$ Torr) at room temperature. Excitation photons at 266 nm (4.7 eV) are produced by fourth harmonic generation of nanosecond laser pulses from a Nd:YAG laser or, alternatively, the third harmonic generation of an amplified femtosecond Ti:sapphire laser system. The femtosecond UV laser pulse width is measured to be 150 fs

* Corresponding author. E-mail: wayne.hess@pnl.gov. Phone: 1-509-376-9907.
[†] Pacific Northwest National Laboratory.
[‡] University College London.

10.1021/jp064092b CCC: $33.50 

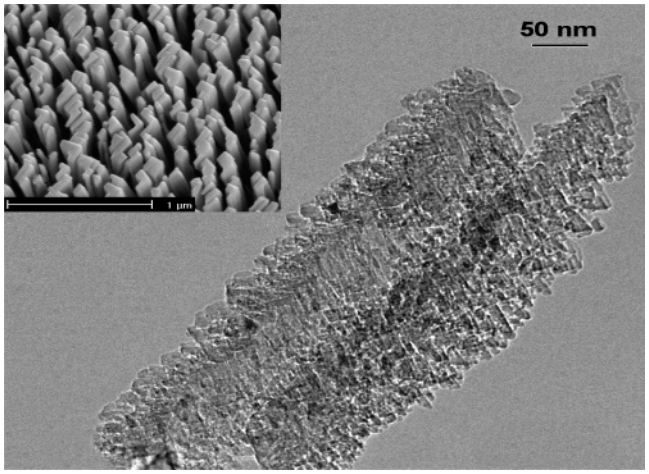


**Figure 1.** Bright-field transmission electron microscope (TEM) image of two MgO columns of an RBD-grown MgO film. The inset displays a scanning electron microscope (SEM) image showing the top view of the same RBD-grown MgO film. RBD-grown films consist of highly porous columns with large numbers of low-coordinated sites.

using a third-order correlation technique and assuming a Gaussian pulse profile. $Mg^0$ atoms emitted from the MgO sample are photoionized by a delayed ionization laser focused approximately 0.4 cm above the sample surface and oriented parallel to it. The ionization laser is a frequency-doubled Nd:YAG pumped dye laser, tuned to the Mg $3s^2\ ^1S_0 \rightarrow 3s3p\ ^1P_1$ transition at 285 nm. Ultrasensitive detection of $Mg^0$ atoms is accomplished using a (1+1) resonance-enhanced scheme and subsequent analysis by time-of-flight mass spectrometry. Velocity profiles are obtained by measuring the relative $Mg^0$ yield as a function of delay between excitation and ionization lasers. The velocity profiles are then transformed to kinetic energies by application of an appropriate Jacobian transformation. All experiments are performed at low fluence ($<3$ mJ/cm$^{-2}$) and repetition rate (20 Hz) using photon energies well below the bulk band gap; therefore, minimal sample heating is expected.

The time-resolved desorption experiments utilize the third harmonic of the femtosecond Ti:sapphire laser system which is split into two pulses of nearly equal intensity. Initially, a single 4.7 eV femtosecond pulse excites the MgO sample. The second time-delayed pulse is overlapped spatially with the first pulse on the MgO surface, causing $Mg^0$ emission. The $Mg^0$ is then detected according to the ionization scheme described above as a function of the delay ($\Delta t$) between femtosecond pulse pairs. The intensities of each femtosecond pulse are adjusted to be slightly above threshold for $Mg^0$ detection to optimize the signal-to-noise ratio. More detailed experimental descriptions have been reported previously.[21,22]

To grow crystalline MgO samples with a high concentration of 3C sites, we use reactive ballistic deposition (RBD). The RBD films are grown to a thickness near 600 nm on cleaved LiF crystals, resulting in highly textured films of MgO columns with a large surface area (750−1000 m$^2$/g).[23] The stoichiometry and crystallographic orientation of RBD-grown films has been verified by X-ray photoelectron spectroscopy and X-ray diffraction.[20]

### 3. Experimental Results

Figure 1 shows electron micrograph images of RBD-grown MgO exhibiting a large number of low-coordinated surface sites. In particular, the number of 3-coordinated (3C) surface sites such as corners, kinks, and step corners are accentuated relative to a pristine single crystal. MgO samples with a large number of 3C sites, such as RBD-grown films, readily emit Mg atoms following low fluence 4.7 eV excitation using either nanosecond or femtosecond pulses. In fact, at low laser power, it is possible to desorb Mg atoms without simultaneously desorbing either $Mg^+$ or $Mg^{2+}$ ions. Previous nanosecond pulse experiments have demonstrated that a large fraction of Mg atoms desorb with hyperthermal energies.[5]

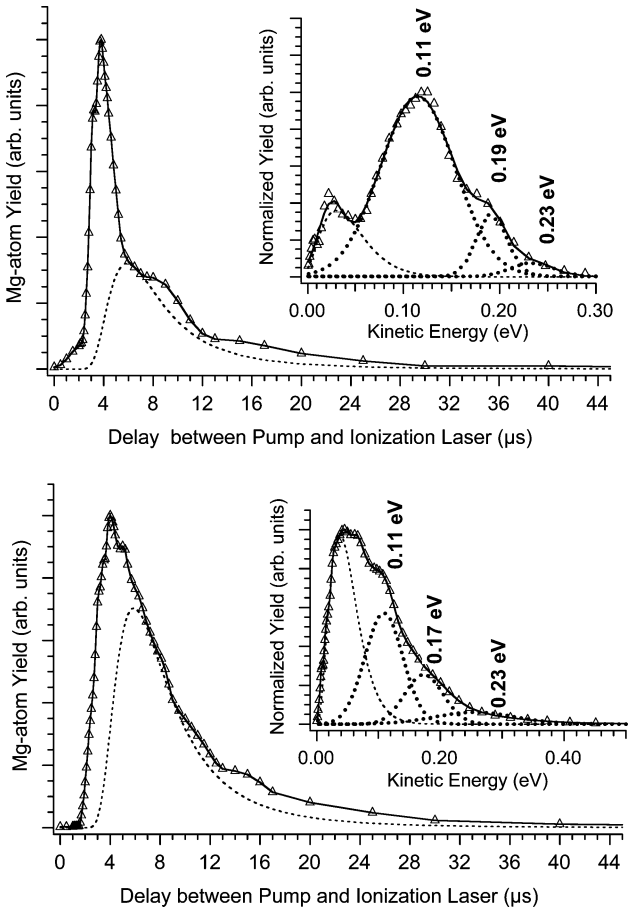


**Figure 2.** Velocity profiles and kinetic energy distributions of $Mg^0$ atoms from an RBD-grown MgO film following irradiation using nanosecond (upper) and femtosecond (lower) excitation pulses at 4.7 eV. The insets show the corresponding $Mg^0$-atom kinetic energy distributions obtained by transformation of the velocity profiles; hyperthermal components at ~0.11, ~0.18, and ~0.25 eV are evident. The dotted line in the velocity profiles represents a Maxwell−Boltzmann fit of the thermal emission component ($T = 300$ K).

Figure 2 displays the velocity profiles obtained by measuring the relative $Mg^0$ yield as a function of the delay between excitation and ionization lasers following 4.7 eV nanosecond (upper panel) and femtosecond (lower panel) excitation. The resulting kinetic energy distributions demonstrate significant hyperthermal components with distinct peaks centered at ~0.11, ~0.18, and ~0.23 eV for both nanosecond and femtosecond pulse excitation (Figure 2). The $Mg^0$ velocity distributions also contain a significant thermal component that likely originates within the bulk of the MgO sample. Here, we focus on the *hyperthermal* $Mg^0$ emission mechanism. Hyperthermal emission originates from the sample surface (or near surface) as diffusion of Mg atoms from the bulk leads to thermal kinetic energy distributions under our experimental conditions. Our ab initio theoretical calculations[4−6] predict that selective excitation of 3C sites creates localized excitons that subsequently induce desorption of hyperthermal neutral O and Mg atoms.

A significant feature in Figure 2 is the existence of three different hyperthermal energies for the desorbing $Mg^0$ atoms

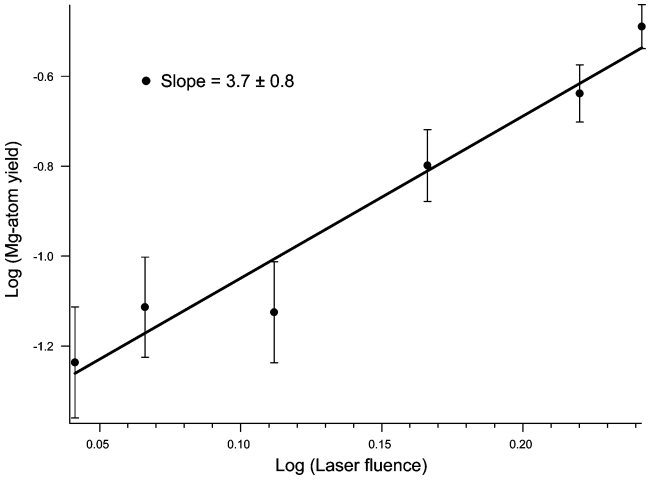


**Figure 3.** Hyperthermal $Mg^0$ yield as a function of femtosecond laser fluence in the low fluence regime below the ablation threshold using 4.7 eV excitation. The reported uncertainty represents only the $2\sigma$ statistical error from the linear least-squares fit.

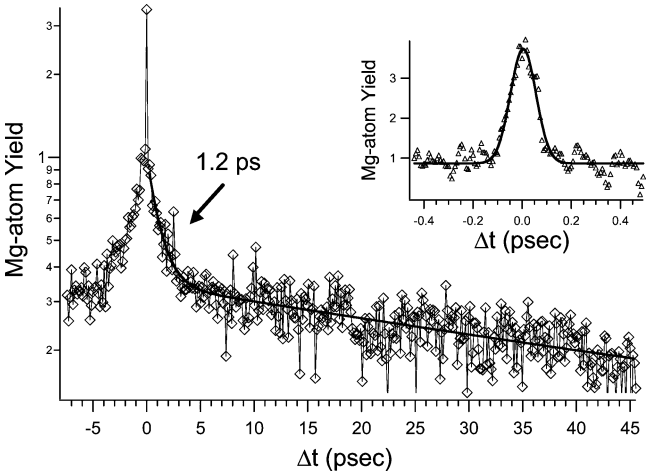


**Figure 4.** Time-resolved correlation measurement of the $Mg^0$-atom yield induced by paired 4.7 eV femtosecond pulses displayed in semilog format. The $Mg^0$-atom yield is plotted versus the delay between femtosecond pulse pairs ($\Delta t$). A constant offset common in two-pulse correlation experiments has been subtracted from the data for clarity. The inset displays the expanded region near $\Delta t = 0$ showing the pulse-width-limited response.

following both nanosecond and femtosecond excitation. Previous nanosecond desorption measurements have suggested that these three components originate from different types of 3C sites, that is, corners, kinks, and step corners.[5,6] The fact that these components appear with nearly identical energies following either nanosecond or femtosecond excitation supports the argument that desorption occurs from the same set of 3C sites in both cases. The difference in kinetic energies is attributed to the difference in local atomic structure of various 3C sites.

Figure 3 displays a representative plot of the hyperthermal $Mg^0$ yield as a function of laser fluence in the low fluence regime slightly above the detection threshold. The Mg-atom yield is found to obey a nonlinear dependence on the excitation laser fluence, $P^n$, with $n = 3.7 \pm 0.8$. Measurement of highly nonlinear power dependences frequently suffers from large systematic and statistical errors. Nonetheless, it is clear that the power dependence is greater than quadratic, and likely between three and four. The nonlinear power dependence demonstrates that multiple excitations are required in order to achieve hyperthermal Mg-atom desorption.

To gain further insight into the mechanism of hyperthermal Mg emission, we have performed femtosecond pump−probe experiments to measure desorption dynamics directly. The time delay of the ionization laser is set to the maximum of the hyperthermal Mg-atom yield, thus ensuring that primarily hyperthermal Mg dynamics are measured. Figure 4 shows the results of such a two-pulse correlation experiment and clearly indicates three time regimes in the Mg hyperthermal emission yield. The first regime is characterized by a pulse-width-limited feature, which is observed only when the two pulses coincide in time (coherence feature). The second and third regimes comprise a 1.2 ps decay feature and a relatively weak longer-lived decay component. Because of the weak signal of the longer-lived component, there is significant scatter in the data, but we estimate that this component has a lifetime of 100 ± 50 ps.

## 4. Discussion

Since crystalline MgO consists of doubly charged $O^{2-}$ ($2p^6$) and $Mg^{2+}$ ($3s^0$) ions, desorption of neutral $O^0$ or $Mg^0$ atoms requires that at least two electrons are transferred between ions, either in a simultaneous two-electron transition or in sequential single-electron transitions. It is clear from Figure 4 that a majority of the Mg hyperthermal yield results from the correlated overlap of the two pulses at zero time delay. This implies that Mg-atom desorption induced by individual femtosecond pulses (as in Figures 2 and 3) results from the simultaneous, or near-simultaneous, displacement of two electrons to the $Mg^{2+}$ site within the 150 fs pulse. The results in Figure 4 also reveal, however, that additional paths lead to hyperthermal $Mg^0$ emission—there are at least two slower dynamical processes characterized by the 1.2 ps and longer (∼100 ps) decay times. We note that further excitation of the longer-lived states may therefore be a part of the mechanism of Mg desorption using weak nanosecond pulses.[5] Since the longer-lived state persists for 100 ps or more, a nanosecond pulse can both initially excite the sample and then further excite the resulting state through subsequent photon absorption.

With the aid of calculations, two different models have been developed to describe the hyperthermal emission of Mg atoms following nanosecond 4.7 eV excitation:[5]

**(i) Bi-exciton Model.** 4.7 eV photoexcitation causes the transfer of one electron from a 4-coordinated $O^{2-}$ ion to the adjacent 3-coordinated $Mg^{2+}$ ion site ($Mg^{2+}_{3C}$). The resulting exciton ($Mg^+-O^-$) may relax to its lowest triplet excited state, accompanied by 1.2 Å displacement of the corner $Mg^+$ ion out of the surface along the ⟨100⟩ axis. Further excitation with a second 4.7 eV photon either ionizes the first excited state or excites the system to a transiently bound higher excited state, which then relaxes with spontaneous desorption of $Mg^0$ with a kinetic energy near 0.3 eV.

$$Mg^{2+}_{3C}-O^{2-}_{4C} \xrightarrow{4.7\ eV} \underset{1.Exciton}{Mg^{+}_{3C}-O^{-}_{4C}} \xrightarrow{4.7\ eV} \underset{2.Exciton}{Mg^{0}_{3C}-O^{0}_{4C}} \Rightarrow Mg^0$$

Here and below, it is understood that the $O_{4C}$ symbol represents the three 4-coordinated oxygen ions near the $Mg^{2+}_{3C}$ site.

**(ii) Electron Plus Exciton Model.** In this model, 4.7 eV photons can photoionize the intermediate ($Mg^+-O^-$) exciton state in mechanism (i) or else photoionize a 3C $O^{2-}$ site. In either case, this requires two photons and leads to the formation of a "free" electron. Remote 3C $Mg^{2+}$ sites have a positive electron affinity and therefore can attract and trap a free electron to become a 3C $Mg^+$ site. The resulting $Mg^+-O^{2-}$ state can

be either ionized or further excited by a third 4.7 eV photon. In the latter case, an electron from the 4C $O^{2-}$ ion site is transferred to the 3C $Mg^+$ site, followed by exciton relaxation and spontaneous $Mg^0$-atom emission with a kinetic energy near 0.2 eV.

$$Mg^{2+}_{3C}-O^{2-}_{4C} + e^- \rightarrow Mg^{+}_{3C}-O^{2-}_{4C} \xrightarrow{4.7\ eV} Mg^{0}_{3C}-O^{-}_{4C} \Rightarrow Mg^0$$
Exciton

The proposed models provide a basis for understanding the observed Mg-atom desorption dynamics. Model (i) predicts a quadratic power dependence, while the "electron plus exciton" model (ii) predicts a three-photon dependence. Our previous nanosecond laser results suggest that the observed three-photon power dependence[5] is most consistent with mechanism (ii). The femtosecond laser Mg-atom power dependence is clearly greater than quadratic, and within error limits of $n = 3$ as model (ii) predicts. Therefore, the electron plus exciton model is consistent with both femtosecond and nanosecond laser experiments.

According to the electron plus exciton model, excitation of MgO samples prepares $Mg^+-O^{2-}$ species through photogeneration of an electron followed by its trapping at 3C $Mg^{2+}$ sites. This electron trapping is accompanied by a strong (and presumably rapid) lattice relaxation;[5] however, it is plausible that this $Mg^+-O^{2-}$ species can be further photoexcited to produce hyperthermal $Mg^0$ *before* the lattice relaxation is complete. Our preliminary calculations demonstrate that 4.7 eV excitation has a higher excitation probability for unrelaxed rather than relaxed 3C $Mg^+$ sites. Therefore, structural relaxation of 3C $Mg^+$ sites can lead to a decrease of $Mg^0$ emission and the 1.2 ps decay may represent the relaxation time of the 3C $Mg^+$ site. The ionization energy of the relaxed 3C $Mg^+$ site is about 1.0 eV.[5] Therefore, the lifetime of this relaxed 3C $Mg^+$ state, with respect to its thermal or photoinduced ionization, can be sufficiently long that, under nanosecond excitation, another photon may be absorbed from the pulse, leading to hyperthermal $Mg^0$ emission. Thus, it is reasonable to associate the 1.2 ps decay with 3C $Mg^+$ site relaxation and the longer-lived 100 ps decay with the 3C $Mg^+$ lifetime. Recent experimental[24] and theoretical[25] results for ionic solids both indicate displacement time scales similar to those described here. We note that the different types of 3C sites evident in the kinetic energy distributions all contribute to the observed dynamics and that it is not possible to equate different time scales with different sites within the context of the model. This interpretation implies that the lifetime of anion excitons, that can be ionized and give rise to $Mg^+$ corners, is much longer than 100 ps and their population remains constant over the short time scale shown in Figure 4.

We note that the temporal resolution of the coherence feature is limited by the pulse width; that is, the 150 fs time scale represents an upper limit. In any case, the coherence feature corresponds to an extremely fast process, which may not involve relaxation of the initially formed singlet exciton to the triplet state, as required by the bi-exciton model (i) or electron transfer from remote surface traps, as required by the electron plus exciton model (ii). Instead, it can originate from desorption induced by multiphoton "on-site" transitions in the vicinity of the 3C Mg site. In this case, the 150 fs feature and the longer-time features in Figure 4 would correspond to unrelated processes.

**Acknowledgment.** The authors were supported by the Department of Energy, Divisions of Chemical Sciences of the Office of Basic Energy Sciences. Pacific Northwest National Laboratory is operated for the U.S. Department of Energy by Battelle. Experiments were performed in the Environmental Molecular Sciences Laboratory, a U.S. Department of Energy user facility operated by the office of Biological and Environmental Research. P.V.S. is supported by the Grant-in-Aid for Creative Scientific Research (Grant No. 16GS0205) from the Japanese Ministry of Education, Culture, Sports, Science and Technology.

## References and Notes

(1) *Femtosecond Chemistry*; Manz, J., Woste, L., Eds.; VCH: Weinheim, Berlin, 1995; Vols. I−II.

(2) Zewail, A. H. *J. Phys. Chem. A* **2000**, *104*, 5660.

(3) *Femtochemistry and Femtobiology*; Sundstrom, V., Ed.; World Scientific: Singapore, 1997.

(4) Hess, W. P.; Joly, A. G.; Beck, K. M.; Henyk, M.; Sushko, P. V.; Trevisanutto, P. E.; Shluger, A. L. *J. Phys. Chem. B* **2005**, *109*, 19563.

(5) Beck, K. M.; Henyk, M.; Wang, C.; Trevisanutto, P. E.; Sushko, P. V.; Hess, W. P.; Shluger, A. L. *Phys. Rev. B* **2006**, *74*, 045404.

(6) Trevisanutto, P. E.; Sushko, P. V.; Shluger, A. L.; Beck, K. M.; Henyk, M.; Joly, A. G.; Hess, W. P. *Surf. Sci.* **2005**, *593*, 210.

(7) Zecchina, A.; Lofthouse, M. G.; Stone, F. S. *J. Chem. Soc., Faraday Trans. 1* **1975**, *71*, 1476.

(8) Spoto, G.; Gribov, E. N.; Ricchiardi, G.; Damin, A.; Scarano, D.; Bordiga, S.; Lamberti, C.; Zecchina, A. *Prog. Surf. Sci.* **2004**, *76*, 71.

(9) Coluccia, S. *Stud. Surf. Sci. Catal.* **1985**, *21*, 69.

(10) Coluccia, S.; Barton, A.; Tench, A. *J. Chem. Soc., Faraday Trans. 1* **1981**, *77*, 2203.

(11) Coluccia, S.; Deane, A. M.; Tench, A. *J. Chem. Soc., Faraday Trans. 1* **1978**, *74*, 2913.

(12) Coluccia, S.; Tench, A.; Segall, R. L. *J. Chem. Soc., Faraday Trans. 1* **1979**, *75*, 1769.

(13) Diwald, O.; Sterrer, M.; Knözinger, E.; Sushko, P. V.; Shluger, A. L. *J. Chem. Phys* **2002**, *116*, 1707.

(14) Sterrer, M.; Diwald, O.; Knözinger, E.; Sushko, P. V.; Shluger, A. L. *J. Phys. Chem. B* **2002**, *106*, 12478.

(15) Ermer, D. R.; Shin, J.-J.; Langford, S. C.; Hipps, K. W.; Dickinson, J. T. *J. Appl. Phys.* **1996**, *80*, 6452.

(16) Ermer, D. R.; Langford, S. C.; Dickinson, J. T. *J. Appl. Phys.* **1997**, *81*, 1495.

(17) Garrone, F.; Zecchina, A.; Stone, F. S. *Philos. Mag. B* **1980**, *42*, 683.

(18) Shluger, A. L.; Sushko, P. V.; Kantorovich, L. N. *Phys. Rev. B* **1999**, *59*, 2417.

(19) Sushko, P. V.; Shluger, A. L. *Surf. Sci.* **1999**, *421*, 157.

(20) Henyk, M.; Beck, K. M.; Engelhard, M. H.; Joly, A. G.; Hess, W. P.; Dickinson, J. T. *Surf. Sci.* **2005**, *593*, 242.

(21) Beck, K. M.; Taylor, D. P.; Hess, W. P. *Phys. Rev. B* **1997**, *55*, 13252.

(22) Beck, K. M.; Joly, A. G.; Hess, W. P. *Surf. Sci.* **2000**, *451*, 166.

(23) Dohnálek, Z.; Kimmel, G. A.; McCready, D. E.; Young, J. S.; Dohnálková, A.; Smith, R. S.; Kay, B. D. *J. Phys. Chem. B* **2002**, *106*, 3526.

(24) Tanimura, K.; Hess, W. P. *Phys. Rev. B* **2004**, *69*, 155102.

(25) Williams, R. T.; Song, K. S. *Surf. Sci.* **2005**, *593*, 89.